# Laser requirements and advances for Raman techniques

Andreas Isemann
Laser Quantum GmbH, 78467 Konstanz, Germany

## INTRODUCTION

Raman scattering as a probe of vibrational transitions has made leaps and bounds since its discovery, and various schemes based on this phenomenon have been developed with great success.

Applications range from basic scientific research, to medical and industrial instrumentation. Some schemes utilise linear Raman scattering, whilst others take advantage of high peak-power fields to probe nonlinear Raman responses.

This article intends to provide a brief overview of the differences and benefits, together with the laser source requirements and the advancements in techniques enabled by recent developments in lasers.

## LINEAR RAMAN

The advent of the laser in providing a high-intensity coherent light source has helped to make Raman scattering a useful method for spectroscopy by increasing signal levels of the spontaneous event to enable use of readily available detectors.

The most widely used method to date is linear Raman, which takes advantage of commercial continuous-wave lasers. The choice of excitation wavelength depends on the sample used, where in general, a shorter wavelength would yield a higher efficiency yet suffers from higher scattering and may induce damage in biological samples within the UV region.

A diode pumped solid state (DPSS) laser with a wavelength between 473 nm and 1064 nm, a narrow bandwidth output of few tens of GHz or below 1 MHz if needed within the linewidth of vibrational transitions for high resolution, low noise (less than 0.02%) and excellent beam quality (fundamental transversal electromagnetic mode TEM00) provides optimised performance for the resolution of the Raman measurement needed.

The wavelength is chosen based on the sample under investigation, with 532 nm being commonly used for the necessary virtual electronic transition. In the following section, four examples from different areas of Raman applications show the diverse applications of linear Raman and what advances have been achieved.

An example of studying a real-world application, the successful control of food quality using Raman spectroscopy and multivariate analysis, is described by Jernshøj *et al.*[1]. Examining the quality of meat and vegetables is discussed, together with the source specification, when constructing a system for conditions outside of a laboratory environment.

For real-world applications, the laser source needs not only to work at the right output parameters, but also it necessitates a robust design making it portable and highly efficient for integration into instruments and being able to interface with operating software.

The two next experiments benefit from the high resolution that a narrow linewidth laser source offers as well as its high beam quality.

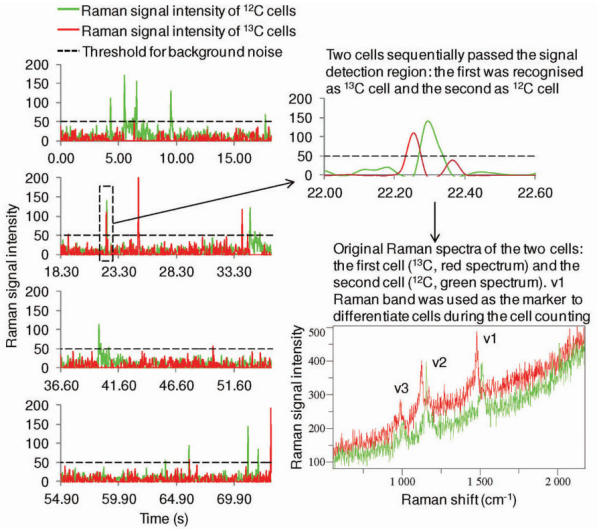


**FIGURE 1** An example of the RR microfluidic device counting of photosynthetic microorganisms. As the cells of the model strain Synechocystis sp. PCC 6803 flow through the Raman detection area of the microfluidic device, RR spectra were acquired continuously about 27 times every second. The v1 RR band was used to differentiate 12 C- and 13 C-cells. The intensity of this band was plotted against the temporal axis and displayed in green and red for 12 C- and 13 C-cells, respectively. A part of the figure near 23.3 s was enlarged to show a 13 C- and 12 C-cell passed through the Raman detection area sequentially only about 0.1 s apart from each other; the untreated RR spectra of those two cells show a distinctive red shift of all of the carotenoids RR bands.
*Reprinted (adapted) with permission from Li et al[2]. Copyright (2012) American Chemical Society*



AM

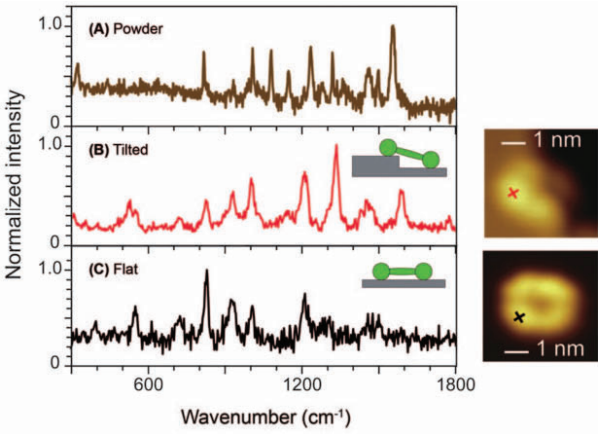


**FIGURE 2** Single-molecule TERS of a porphyrin derivate examined with UHV-STM at low temperatures. (A) The Raman spectrum from powder represents many orientations, whereas (B) TERS was able to resolve a molecule tilt, and (C) also shows single-molecule resolution on a flatly oriented molecule. Especially the differences between TERS spectra (B) and (C) are remarkable. Adapted with permission from Xhang, et al.[8]



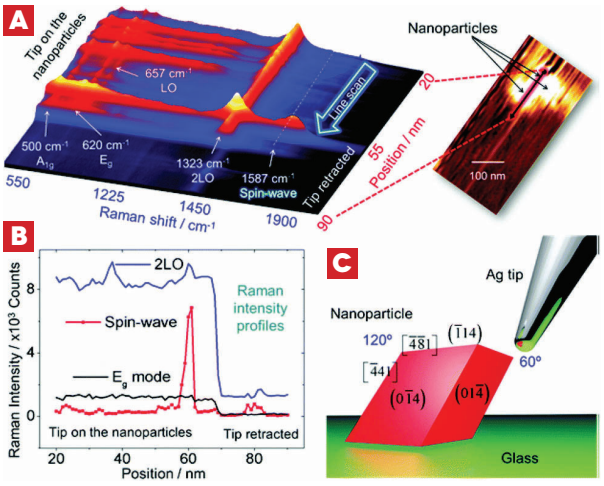


**FIGURE 3** a) Tip-enhanced Raman spectra in a line scan along the nano-particles/glass interface. The stacking representation shows several first order modes below 700 cm–1 , the 2LO mode around 1323 cm–1 and the spin-wave mode around 1587 cm–1 . The step size used to obtain this set of spectra was 1 nm. In the inset is shown the AFM image acquired during the TERS line scan (b) intensity profiles of three modes along the line scan showing the sharp increase in the spin-wave intensity when the TERS tip is on the nanoparticle. This is followed by a decrease in the intensity of all modes when the tip was retracted (tip off). (c) A sketch of the tip–nanoparticle configuration shows the anisotropy between the two sides of the particle with respect to the tip. Crystallographic facets and edges are set according to Rodriguez et al.[27]



Application of a single longitudinal mode (SLM) laser at 532 nm with a linewidth of 1 MHz enables high resolution resonance Raman (RR) spectra from the excitation of carotenoids to differentiate between $^{13}CO_2$ and $^{12}CO_2$, used for high throughput profiling of cell populations[2], see fig. 1. The cells analysed are from photosynthetic microorganisms that are of extraordinary value in the area of renewable energy and biotechnology.

In this research, a high throughput Raman-activated cell sorting (RACS) system has been developed, to perform Raman-activated cell counting. Being able to tightly focus the laser beam provides for necessary spatial resolution in the order of 0.5 - 1 µm to look at individual cells.

A novel approach for precise quantitative measurements of optical mobility in atomically thin films based on high resolution Raman is presented by Ji *et al.*[3]. Using a large change in the intensity of the Raman mode with an applied strong magnetic field that occurs in one plane, but not the out of plane Raman mode. It stems from a magnetic field induced symmetry breaking.

A quantitative analysis of the field dependent Raman intensity allows the determination of the optical mobility. For the quantitative measurements, the low noise and high power stability are important. The excellent beam quality of the SLM laser used (Laser Quantum torus), enables confocal micro-Raman in the measurement setup.

The more commonly used linewidth in continuous wave (CW) Raman is a few 10s of GHz, where most robust lasers are readily available. In cancer research, screening cells for potentially cancerous behaviour calls for an automated analysis system. Such a system based on laser tweezers Raman spectroscopy (LTRS) has been presented by Casabella *et al.*[4]. An excellent beam quality of TEM00 ensuring a tight focus as well as a long-term stable beam pointing are needed for trapping the individual cells in the microfluidic channels and for the Raman measurement.

Two lasers of different wavelength were used (1064 nm for trapping, 532 nm for Raman, both from the Laser Quantum ventus series), which integrated well into the overall system control by use of their remote control capability.

Some samples allow increased efficiency of the scattering when the Raman transition happens to occur close to a real transition. However, not all samples of interest would offer this benefit. To increase the sensitivity and spatial resolution of linear Raman, variations such as surface enhanced Raman scattering (SERS) or as a subvariant, tip enhanced Raman scattering (TERS) have been developed.

In SERS, structured surfaces are used to increase the Raman signal level with the electrical field enhancements due to those structures. Recently, also hybrid structures making use of nano-sized semiconductors, including magnetic materials, have attracted interest due to their excellent SERS performance, as described by Prakash and colleagues[5].

In TERS, the excitation light is brought onto the sample via an atomic force microscope (AFM) tip using plasmonic effects. This helps to overcome the diffraction limit of the laser spot, increasing the spatial resolution, as well as giving a field enhancement due to the tip geometry. In some cases, depending on the sample, the increase of the signal due to the field enhancement overcomes the decrease due to a lower number of oscillators (molecules) inside the excitation volume. An excellent laser beam quality with a high degree of polarization enables it to focus down to a micrometre onto the AFM needle as well as providing efficient excitation of the polarization dependent surface plasmon, the mechanism responsible for electric field enhancement at the tip of the needle. The articles by Kumar[6] and Langelüddecke[7] provide an overview of the method and variety of applications.

As always with input coupling into microscope setups, a superb beam pointing stability with fast warmup times on the order of a few minutes help with reliable day to day operation to concentrate on the experiment.

In the following, two examples of achievements using TERS are given, before turning to non-linear Raman.

The high spatial resolution of TERS has enabled the visualisation of the tilt of a single molecule by means of measuring a spectrum, see figure 2 from the paper by Zhang *et al.*[8] Also, the authors were able to resolve the ring system of a single porphyrin derivative with a spatial resolution of 0.5 nm, see fig. 2 (right side).

In another fascinating experiment, TERS has been able to reveal spin waves in iron oxide nanoparticle, as described by Rodriguez *et al.*[9] and depicted in fig. 3 using micro-Raman experiments.

## NON-LINEAR RAMAN

To drastically increase the efficiency of the Raman process, various coherent (nonlinear) Raman processes have been studied. The Nonlinear Raman process uses at least two different wavelengths, but uses the same Raman active vibrational mode as the linear Raman technique.

Typically, laser setups using two laser beams of different colour and in pulsed mode enable a more elaborate, but coherent process, that generates a signal which is generally orders of magnitude higher. In practise, the advantage of coherent Raman scattering over linear Raman is this overall higher signal.

In Coherent Antistokes Raman Scattering (CARS), the difference between the two wavelengths is used to coherently drive a Raman transition.

Typically, two narrow bandwidth picosecond electronically synchronized laser pulse trains have been used, one of which is scanned in the wavelength to do CARS spectroscopy. The shape of the CARS signal is different from that of linear Raman, also the overall sensitivity is limited by the distinction between the resonant and non-resonant part of the signal. An overview of the method is given in a book by Xie and colleagues[10].

A variant of Coherent Raman is Stimulated Raman Scattering (SRS), which again uses lasers of two different colours with synchronized output pulses to coherently drive a nonlinear process. The advantage is greatly reduced non-resonant background, and that the output trace is the same as conventional Raman allowing existing databases of compound results to be used, as well as quantitative interpretation of the measured data[11].

SRS makes use of modulation of one of the laser beams, a double modulation technique Stimulated Raman Gain and Opposite Loss Detection (SRGOLD) proposes background free detection and is the latest variant using a three colour laser beam excitation scheme[12].

Both CARS and SRS can in principal be done in versions using femtosecond or picosecond lasers (and even nanosecond lasers), each with different advantages and drawbacks. Historically, two electronically synchronized tuneable laser sources have been used[13], or more typically today, optical parametric oscillators, providing optically synchronised pulses.

However, todays available commercial implementations are often hampered with limited tuning speed, and hence slow in acquisition of a CARS/SRS spectrum[14].

One elegant way for considerably increasing the acquisition speed or even enabling single beam capability is the use of multiplex CARS[15,16] or multiplex SRS[17,18]. With this technique, a narrow band pump and a broadband Stokes pulse, or even one ultra-broadband spectrum with phase shaping supply all wavelengths needed to simultaneously record a large number of Raman shifts. However, parallel detection may require dedicated sophisticated detectors and electronics[18].

With extremely broadband laser oscillators offering typical bandwidth on the order of 400 nm in the NIR and also high repetition rate amplified systems like an OPCPA offering a bandwidth of greater 300 nm being readily available, broadband single beam Raman techniques have become possible. The available bandwidth allows a wavenumber range of up to 4000 $cm^{-1}$. It also allows for an efficient combination of multiple modalities, or for very fast spectroscopic CARS modality using a quite simple detector in form of a photo diode.

One implementation of CARS using broad bandwidth uses the principle of spectral focussing[19]. A simple implementation relying on glass stretchers to measure two vibrational frequencies with two (or more) pairs of pump/stokes pulses simultaneously is called differential CARS (or D-CARS). One advantage of this method is the fast acquisition speed of a few seconds for complete images and the effectively rejection of non-resonant background using the D-CARS signal. The simple analysis scheme allows for rapid distinguishing between saturated and unsaturated lipids[20].

The laser source providing a sufficiently large bandwidth not only enables single beam CARS, but also has been used in a multimodal, or hyperspectral scheme combining D-CARS covering a wavenumber range of 2600 $cm^{-1}$ with a resolution of 10 $cm^{-1}$ together with second harmonic generation (SHG) as well as two photon fluorescence (TPF) imaging – all from a single beam at the same time, using a pulse shaper[21,22]. An example image is given in fig. 4 providing much richer information than from one imaging modality alone.

An early implementation of spectral focusing using an octave spanning oscillator (Laser Quantum venteon) and a spatial light modulator to do single-pulse (single beam) CARS microscopy is described by Isobe et al[23]. In fig. 5, CARS images of unstained HeLa cells are shown from this experiment demonstrating the applicability to biological samples.

The use of an octave spanning oscillator allowed the researchers to focus into narrow spectral regions ranging from approx. 1000 $cm^{-1}$ to 4800 $cm^{-1}$.

Aimed at fast measurement of spectroscopic CARS, the method of Fourier Transform (FT) CARS shows great potential. The principle has been shown by Ogilve et al[24] using a 100 MHz oscillator and is based on a pump probe type dual pulse setup.

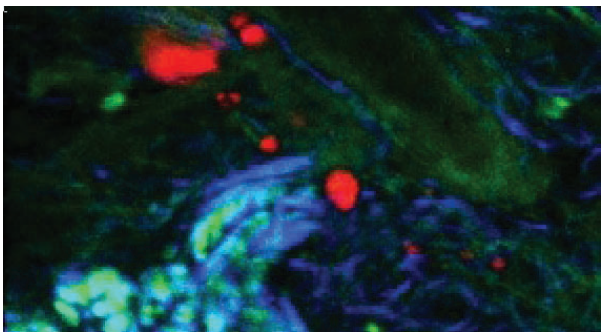

**FIGURE 4** TPF (green), CARS from subcutaneous lipid deposits (red) and SHG from collagen (blue) of tissue from a mouse tail

*Reprinted (adapted) with permission from by Pope et al.[9] Copyright (2013) Optical Society of America*

In this method, the CARS spectrum is obtained through the Fourier transform of the CARS interferogram – i.e. the CARS emission as a function of time delay between two identical collinear excitation pulse trains with a generated time delay between successive pulses.

The non-resonant background can be removed by simply removing the contribution around zero time delay. The detection of the CARS signal can be accomplished with a simple Si-diode.

Using a 5 fs oscillator with a spectral bandwidth of 4000 $cm^{-1}$ the applicability of FT CARS to biological samples covering the bandwidth in a single measurement has been demonstrated[23]. An image of unstained HeLa cells has been obtained by FT CARS (fig. 6) shows the differentiating of mitochondria or endoplasmic reticulum, the nucleus and water.

The speed of the acquisition of a complete CARS spectrum using FT CARS depends on how fast the two pulses can pass through the needed delay times that contribute to the CARS interferogram.

The refresh time then depends on how fast this cycle can be repeated. The time delays which contribute to the interferogram depend on the dephasing time of the coherent Raman excitation, which is typically on the picosecond (ps) timescale. The interferometric, non-resonant background being present at short delay times only and hence can be completely suppressed by suitably positioning the numerical apodization window[26].

In the implementation of the work published by Isobe and colleagues a mechanical delay line is used[23]. The first step to speed up the measurement is to use an ASynchronous OPtical Sampling (ASOPS) dual comb type setup where two repetition rate

locked laser oscillators with a slight offset in their repetition rate are used to generate the pulse pair[24]. In this scenario, the refresh time is given by the inverse of the laser repetition rate. The measurement time of one scan depends on how fast the delay of the two pulses covers the timeframe of the interferogram.

The benefit of using oscillators with 1 GHz repetition rate over a 100 MHz repetition rate in the implementation from Ideguchi[25] is a 10 times higher refresh rate, i.e. 10 times higher duty cycle - number of measurements for the same integration time - as well as much higher density of sampling steps at the same difference in repetition rates. In other words, using GHz repetition rates, at the same sampling step size, one can operate at much higher refresh times, i.e. more measurements per unit time. The fast acquisition time with a high refresh rate enables the measurement of transients or short lived species.

Recently, a first implementation of such a dual comb CARS system using two GHz oscillators has been demonstrated[26]. The bandwidth of the emitted pulses is 60 nm which allows for sub-20 fs compressed pulses. They enabled measurements with a span from 400 - 1400 $cm^{-1}$ and a resolution of 6 $cm^{-1}$ given by the time window of the Fourier transformation, at a kHz refresh rate with the actual acquisition time of one scan as short as 5 µs.

To demonstrate that this method can measure at sufficient resolution to discriminate different substances, a spectrum of a mixture of toluene, chloroform and cyclohexane has been taken, see fig. 7. The two neighbouring peaks of toluene and cyclohexane are only 13 $cm^{-1}$ apart, yet clearly resolved. The measurement revealed a linear dependency of the line maximum with concentration as well as pulse energy, which will be helpful looking towards quantitative analysis. The use of oscillators with sub-20 fs allows to extend the setup with multimodal or hyperspectral capabilities.

## CONCLUSIONS

In conclusion, a selection of linear Raman applications has been presented that make use of the excellent beam quality and beam pointing and power stability with low noise of modern laser sources as well as to the narrow linewidth properties where applicable.

A high efficiency, robustness and remote operation capability benefits all applications, these being a prerequisite for integration into industrial or automated systems.

The availability for broadband pulsed laser sources covering spectra of several hundred nm have enabled fast coherent Raman measurements as well as enabling multimodality efficiently. Finally, Fourier Transform CARS in combination with dual comb technology enables fast spectroscopic CARS measurements within microseconds. The use of GHz repetition rate oscillators provides for a factor of 10 higher refresh rates of the spectral acquisition compared to commonly available 100 MHz oscillators.

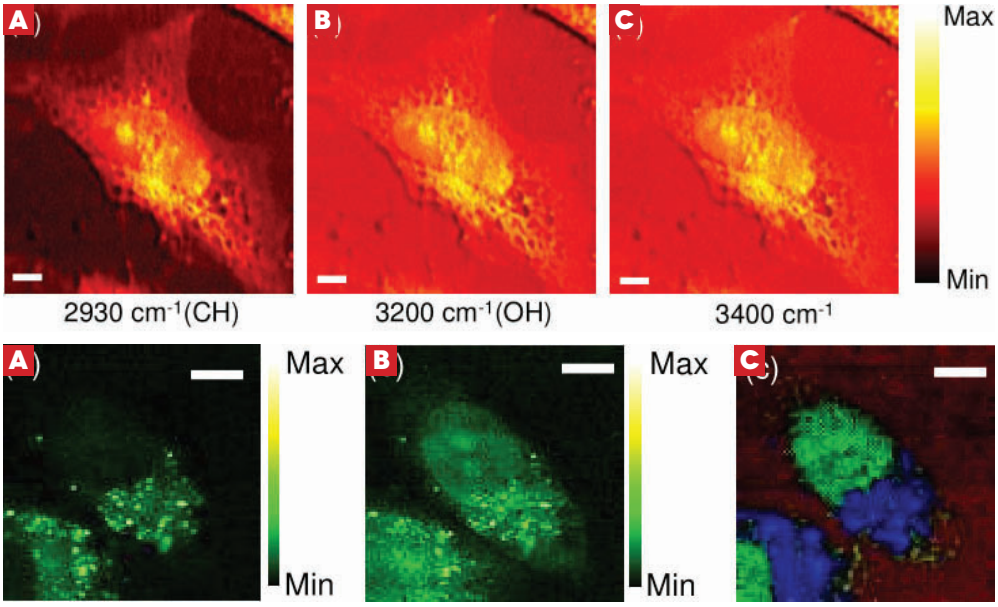


**FIGURE 5**, top, CARS images of an unstained HeLa cell by selective excitation at 2930 cm–1 (a), 3200 cm–1 (b) and 3400 cm–1 (c). Scale bar is 6 µm. *Reprinted (adapted) with permission from Isobe et al[23]. Copyright (2009) Optical Society of America*

**FIGURE 6**, above, (a, b) CARS images of an unstained HeLa cell constructed from integration in the spectral bands of 2800-2900 cm–1 (a), and 2900-3000 cm–1 (b). (c) Combined image of three CARS images of an unstained HeLa cell reconstructed after the NSC process using the CARS spectrum from mitochondria or endoplasmic reticulum (blue), the nucleus (blue) and water (red). Scale bar is 8 µm. *Reprinted (adapted) with permission from Isobe et al[23]. Copyright (2009) Optical Society of America*

## REFERENCES


1 K. Jernshøj, S. Hassing, L. Christensen, A Non-Destructive and On-site Tool for Control of Food Quality ?, *Food Quality*, Kostas Kapiris. InTech - Open Access Publisher, (2012) 47-72.

2 M. Li, P. Ashok, K. Dholakia, Wei E. Huang, Raman-Activated Cell Counting for Profiling Carbon Dioxide Fixing Microorganisms, *The Journal of Physical Chemistry* A, 116 (25) (2012) 6560-6563.

3 J. Ji, A. Zhang, J. Fan, Y. Li, X. Wang, J. Zhang, E. Plummer, Q. Zhang, Giant magneto-optical Raman effect in a layered transition metal compound, *PNAS*, 113(9) (2016) 2349-2353.

4 S. Casabella, P. Scully, N. Goddard, P. Gardner, Automated analysis of single cells using Laser Tweezers Raman Spectroscopy, *Analyst*, 141 (2016) 689.

5 O. Prakash, S. Kumar, P. Singh, V. Deckert, S. Chatterjee, A. Ghosh, R. Singh, Surface-enhanced Raman scattering characteristics of CuO : Mn/Ag heterojunction probed by methyl orange: effect of Mn2+ doping, *Journal of Raman Spectroscopy*, 47 (2016) 813–818.

6 N. Kumar, S. Mignuzzi, W. Su, D. Roy, Tip-enhanced Raman spectroscopy: principles and applications, *J EPJ Techniques and Instrumentation* D, 2(1) (2015).

7 L. Langelüddecke, P. Singh, V. Deckert, Exploring the Nanoscale: Fifteen Years of Tip-Enhanced Raman Spectroscopy, *Applied Spectroscopy* 69(12) (2015) 1357 - 1371.

8 R. Zhang, Y. Zhang, Z.C. Dong, S. Jiang, C. Zhang, L.G. Chen, L. Zhang, Y. Liao, J. Aizpurua, Y. Luo, J.L. Yang, J.G. Hou, Chemical Mapping of a Single Molecule by Plasmon-Enhanced Raman scattering, *Nature* 498(7452) (2013) 82-86.

9 R. Rodriguez, E. Sheremet, T. Deckert-Gaudig, C. Chaneac, M. Hietschold, V. Deckert, D. Zahn, Surface- and tip-enhanced Raman spectroscopy reveals spin-waves in iron oxide nanoparticles *Nanoscale* 7 (2015) 9545-9551.

10 X. Xie, J.-X. Cheng, E. Potma, Coherent Anti-Stokes Raman Scattering Microscopy, *Handbook of Biological Confocal Microscopy, Third Edition*, edited by James B. Pawley, Springer Science+Business Media, LLC, New York, 33 (2006) 595-606.

11 P. Nandakumar, A. Kovalev, A. Volkmer, Vibrational imaging based on stimulated Raman scattering microscopy, *New Journal of Physics* 11 (2009) 033026.

12 P. Berto, E. R. Andresen, H. Rigneault, Background free stimulated Raman spectroscopy and microscopy, *Physical Review Letters* 112 (2014) 053905.

13 E. Potma, D. Jones, J.-X. Cheng, X. Xie, J. Ye, High-sensitivity coherent anti-Stokes Raman scattering microscopy with two tightly synchronized picosecond lasers, *Optics Letters* 27 (2002) 1168-1170.

14 S. Brustlein, P. Ferrand, N. Walther, S. Brasselet, C. Billaudeau, D. Marguet, H. Rigneault, Optical

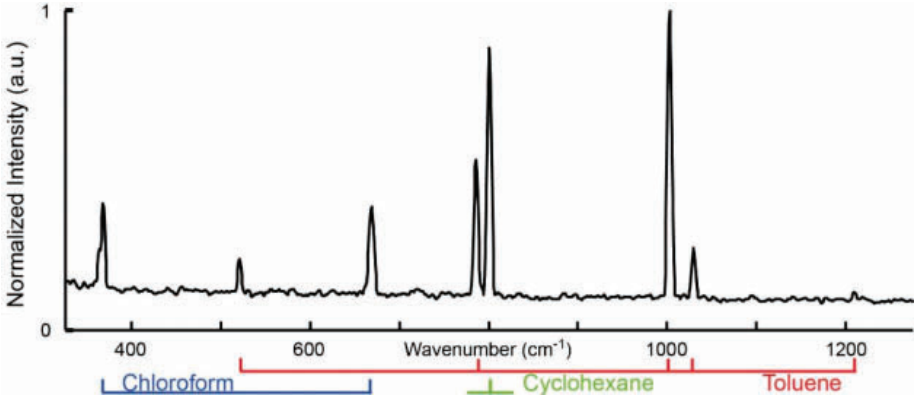


**FIGURE 7** Dual-comb CARS spectrum of toluene, chloroform and cyclohexane with a mixing ratio of 1:1:1. The difference in repetition frequencies is ðf rep. 600 Hz. The apodized resolution is 6 cm–1 and 120 spectra are averaged. The measurement time is 2 ms and the total experimental time is 200 ms.
*Reprinted (adapted) with permission from Mohler et al[26]. Copyright (2013) Optical Society of America*

parametric oscillator-based light source for coherent Raman scattering microscopy: practical overview, *Journal of Biomedical Optics* 16(2) (2011) 021106.
15 J.-X. Cheng, A. Volkmer, L. D. Book, X. Xie, Multiplex Coherent Anti-Stokes Raman Scattering Microspectroscopy and Study of Lipid Vesicles, *The Journal of Physical Chemistry* B 106 (2002) 8493-8498.
16 A. Wipfler, T. Buckup, and M. Motzkus, Multiplexing Single-Beam CARS with Heterodyne Detection, *Applied Physics Letters* 100 (2012) 071102.
17 D. Fu, F.K. Lu, X. Zhang, C. Freudiger, D. R. Pernik, G. Holtom, X. Xie, Quantitative Chemical Imaging with Multiplex Stimulated Raman Scattering Microscopy, *Journal American Chemical Society*, 134 (2012) 3623-3626.
18 C.-S. Liao , M. N. Slipchenko, P. Wang, J. Li, S.-Y. Lee, R. A. Oglesbee, J-X Cheng, Microsecond scale vibrational spectroscopic imaging by multiplex stimulated Raman scattering microscopy, *Light: Science & Applications*, 4 (2015) e265.
19 T. Hellerer, A.M.K. Enejder, A. Zumbusch, Spectral focusing: High spectral resolution spectroscopy with broad-bandwidth laser pulses, *Applied Physics Letters* 85(1) (2004) 25-27.
20 C, Di Napoli, F. Masia, I. Pope, C. Otto, W. Langbein, P. Borri, Chemically-specific dual-differential CARS micro-spectroscopy of saturated and unsaturated lipid droplets, *Journal of Biophotonics* 7(1–2) (2014) 68-76.
21 I. Pope, W. Langbein, P. Watson, P. Borri, Simultaneous hyperspectral differential-CARS, TPF and SHG microscopy with a single 5 fs Ti:Sa laser, *Optics Express* 21(6) (2013) 7096-7106.
22 J. Rehbinder, L. Brückner, A. Wipfler, T. Buckup, M. Motzkus, Multimodal nonlinear optical microscopy with shaped 10 fs pulses, *Optics Express* 22(23) (2014) 28790-28797.
23 K. Isobe, A. Suda, M. Tanaka, H. Hashimoto, F. Kannari, H. Kawano, H. Mizuno, A. Miyawaki, K. Midorikawa, Single-pulse coherent anti-Stokes Raman scattering microscopy employing an octave spanning pulse, *Optics Express* 17(14) (2009) 11259-11266.
24 J. P. Ogilvie, E. Beaurepaire, A. Alexandrou, and M. Joffre, Fourier-transform coherent anti-Stokes Raman scattering microscopy, *Optics Letters* 31(4) (2006) 480-482.
25 T. Ideguchi, S. Holzner, B. Bernhardt, G. Guelachvili, N. Picque, T. W. Hänsch, Coherent Raman spectro-imaging with laser frequency combs, *Nature* 502 (2013) 355-539.
26 K. J. Mohler, B. J. Bohn, M. Yan, G. Mélen, T. W. Hänsch, N. Picque, Dual-comb coherent Raman spectroscopy with lasers of 1-GHz pulse repetition frequency, *Optics Letters* 42(2) (2017) 318-321.
27 R. D. Rodriguez, D. Demaille, E. Lacaze, J. Jupille, C. Chaneac and J.-P. Jolivet, Rhombohedral Shape of Hematite Nanocrystals Synthesized via Thermolysis of an Additive-free Ferric Chloride Solution, *The Journal of Physical Chemistry* C, 111(45) 2007 16866-16870.



## BIOGRAPHY

Dr. Andreas Isemann is Area Sales Manager as well as Business Development Manager with Laser Quantum GmbH. He has studied physics with his initial background in ultrafast lasers from his research in directly diode pumped femtosecond oscillators and amplifiers at the Laser Center Hannover, Germany. With his transition into industry, he has held various positions in sales and marketing as well as product management at Femtolasers GmbH and APE GmbH, before joining Laser Quantum GmbH. One focus has been in application management understanding the requirements on the laser source as well as investigating new applications, which include few cycle pulses, biomedical, as well as non-linear microscopy.

## ABSTRACT

Raman spectroscopy found its place in many areas applying the linear as well as the non-linear implementations of the technique. A summary of the various methods cites selected publications illustrating advances. In the linear case, application profit from industrial grade low noise stable laser sources. In non-linear Raman, availability of ultra-broadband femtosecond laser sources and novel pulse shaping or sampling techniques have enabled new schemes e.g. multiplexing non-linear Raman with second harmonic generation and third harmonic generation giving rich information content, as well as enabling extremely fast acquisition of Raman spectroscopic data within microseconds for investigation of dynamic or transient systems.

## ACKNOWLEDGEMENTS

The author would like to thank Andy Wells, Jennifer Szczepaniak Sloane and Danielle Hardie from Laser Quantum Ltd, Dave Stockwell, PhD from Laser Quantum Inc and Dr. Gregor Klatt from Laser Quantum GmbH for their various contributions.

## CORRESPONDING AUTHOR DETAILS

Andreas Isemann: aisemann@laserquantum.com

**Microscopy and Analysis 31(4): 19-23 (AM), August 2017**